Single adatom adsorption and diffusion on Si(111)-(7×7) surfaces: Scanning tunneling microscopy and first-principles calculations

O. Custance,[1] S. Brochard,[2] I. Brihuega,[1] Emilio Artacho,[1,3] J. M. Soler,[1] A. M. Baró,[1] and J. M. Gómez-Rodríguez[1,*]

[1]*Dept. Física de la Materia Condensada, Universidad Autónoma de Madrid, E-28049-Madrid, Spain*
[2]*Laboratoire de Métallurgie Physique, Unité Mixte de Recherche 6630 du CNRS, Université de Poitiers, SP2M1, Boîte Postale 30179, 86962 Futuroscope Chasseneuil Cedex, France*
[3]*Department of Earth Sciences, University of Cambridge, Downing St., Cambridge CB2-3EQ, United Kingdom*

The adsorption and diffusion of single Pb atoms on Si(111)-(7×7) surfaces have been studied by scanning tunneling microscopy (STM) and first-principles density functional calculations. STM experiments at temperatures from 100 to 130 K have revealed three regions of preferential adsorption, inside each half-unit cell, as well as real time diffusion events between them. The stable adsorption sites have been determined by first-principles calculations and by comparing simulated and measured STM images. The activation barriers for the motion inside the half-unit cells have been calculated and measured experimentally. A very good agreement between calculations and experiments has been found.

Detailed atomic-scale knowledge of adsorption and diffusion mechanisms of single adatoms on highly reconstructed semiconductor surfaces is of fundamental importance for many present and future technological processes. In particular, recent works have unveiled the potentiality, for next generation devices, of self-organized nanoclusters on Si(111)-(7×7).[1–3] However, there is still a lack of both theoretical and experimental information on the stable adsorption sites, diffusion pathways, and energy barriers which are crucial to understand the formation of such nanoclusters.

In the last few years, scanning tunneling microscopy (STM) has become the technique of choice to measure surface diffusion at the atomic scale, nicely complementing the wealth of data from field ion microscopy.[4] STM experiments interpretation, however, generally requires theoretical calculations, ideally from first principles. Such calculations remain a formidable task for highly reconstructed surfaces. The first density-functional theory (DFT) calculations of the Si(111)-(7×7) surface were a landmark in massive parallel computation.[5,6] Further algorithm and hardware improvements have allowed to study this surface with high accuracy.[7] First-principles calculations involving adsorbate adsorption on this surface are, however, still scarce, and even scarcer if including diffusion barriers and pathways [to our knowledge, there is only a very recent report[8] on the analysis of diffusion of Si adatoms on Si(111)-(7×7) surfaces, which appeared after the submission of this study].

In the present work, we have performed combined variable-temperature STM experiments and DFT first-principles calculations of the adsorption and diffusion of single Pb adatoms on Si(111)-(7×7). The motivation for this system was double: on one hand, it is a prototype for a nonreactive interface; on the other hand, there is already some information on it from STM at room temperature (RT).[9–11] These experiments revealed the high mobility at RT of single Pb adatoms within the half-unit cells where they are almost trapped, presenting features that have been found afterwards for other adsorbates such as Tl, Si, Sn, Ag, and

Y.[1,12–15] No previous knowledge existed, however, either on the stable adsorption sites or on the diffusion processes inside the (7×7) half cells, issues which are directly addressed in the present work.

The experiments were carried out in an ultra-high-vacuum (UHV) system (base pressure below 5×10^{-11} Torr) equipped with a variable temperature scanning tunneling microscope (VT-STM), low-energy electron diffraction, Auger Electron Spectroscopy, sample transfer and heating capabilities, a Pb evaporation cell, and a quartz crystal microbalance. Clean reconstructed Si(111)-(7×7) surfaces were obtained by flashing the samples at 1150 °C, after carefully degassing at 600 °C for several hours. The samples were then slowly cooled down to RT and ~ 0.01 monolayer (ML) of Pb was deposited at RT at typical rates of 0.05 ML/min [1 ML is defined as the surface atomic density of the Si(111) surface, i.e., 7.84×10^{14} atoms/cm^2]. The samples were then transferred to the STM and slowly cooled down to temperatures as low as 40 K. The home-built VT-STM instrument is described in detail elsewhere.[16] Connected to a continuous flow liquid He UHV cryostat, it allows imaging at sample temperatures from 40 to 400K. A fully automated electronics, with digital feedback control based on digital signal processor technology, operates the STM.[17] STM data were measured in the constant current mode with sample voltages between -2 and $+2$ V and typical tunnel currents of 100–200 pA.

Figure 1(a) shows a typical STM image measured at RT of a single Pb adatom adsorbed on a Si(111)-(7×7) half-cell. Similar images were already reported for RT.[9–11] The noisy appearance of the Pb-occupied half cell was interpreted as the result of an STM average of the fast thermally activated movement among different adsorption sites. When the sample temperature is lowered enough to make the time scale of this movement compatible with scanning speeds (a few seconds per image), one can resolve individual adatom jumps. This is shown by the sequence in Figs. 1(b)–1(d) of succesive adatom jumps among three different locations inside the half cell, as measured at 108 K. At the relatively high bias voltage used here ($+1.2$ V), the Pb adatoms appear
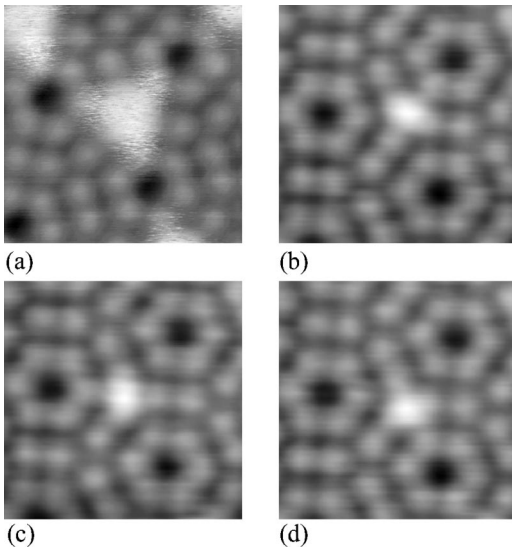
FIG. 1. (a) STM image of Pb/Si(111)-(7×7) measured at room temperature. (b)–(d) Sequence of frames extracted from an STM movie at 108 K illustrating the three main regions that a single Pb atom can occupy inside the (7×7) half-cell. The frame times are (b) $t=0$, (c) $t=74$ s, (d) $t=99$ s. The image size is 4.7 ×4.7 nm^2. Sample bias voltages are 2.0 V (a) and 1.2 V (b)–(d). The tunnel current is 0.2 nA for all images.

as oblong protrusions between two center Si adatoms [Fig. 2(a)]. At the lower bias voltage (+0.5 V) used in Figs. 2(b)– 2(d), they appear as non-symmetric features, not higher than the Si adatoms, the most striking fact being the apparent disappearance (or displacement) of one Si adatom.

More subtle details of the Pb dynamics are revealed by low-bias STM movies. Figure 2 shows three movie frames where, first, the nonsymmetric oblong protrusion seems to oscillate between sites without changing its orientation (b) to (c). It then changes its orientation by 60° (c) to (d). As in high bias movies, three orientations are observed, corresponding to three directions joining two center Si adatoms of the half unit cell. At low bias, however, the protrusion oscillates between two different positions for each orientation, corresponding to the apparent disappearance of one or the other Si adatom.

Two questions arise from the above observations: what are the adsorption sites of Pb adatoms and how do we interpret their complex dynamical behavior. Cho and Kaxiras[18,19]
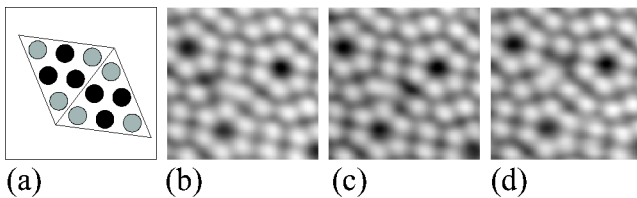

FIG. 2. (a) Schematic drawing of the Si adatoms in the Si(111)-(7×7) unit cell, with center and corner Si adatoms displayed as black and gray circles respectively. (b) to (d) Sequence of frames extracted from an STM movie at 112 K and low sample bias (0.5 V). The frame times are (b) $t=0$, (c) $t=24$ s, (d) $t=216$ s. The image size is 4.8×4.8 nm^2. The tunnel current is 0.2 nA.
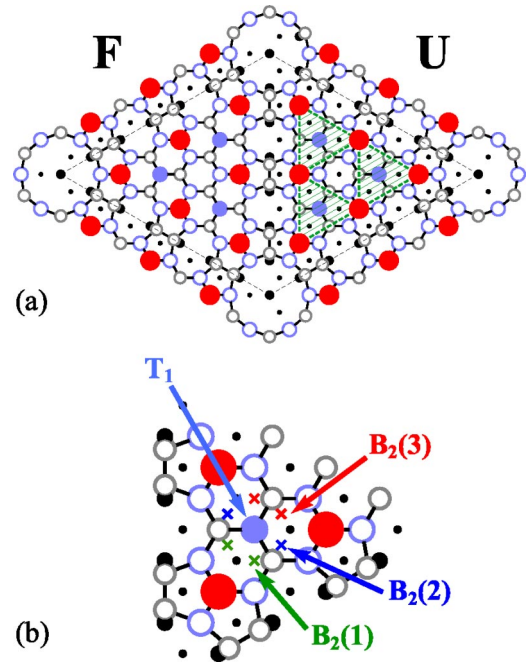

FIG. 3. (a) Schematic drawing of the Si(111)-(7×7) unit cell, where the three basins of attraction of the unfaulted half (U) are marked by shaded triangles. (b) Zoom in of one of those basins, showing the notation for some adsorption sites.

proposed that K, Mg, Ga, Ge, and Si adatoms adsorb most stably on high-coordination sites of the Si(111) reconstruction, rather than on top of the surface dangling bonds. Groups of these high-coordination sites form basins of attraction in which the extra adatoms are localized, with unfrequent jumps to nearby basins. In the (7×7) reconstruction there would be three of these basins per half unit cell. Each one would be roughly limited by two center adatoms and a corner adatom, as outlined in Fig. 3(a). It is worth noting, however, that the calculations of Refs. 18, 19 were performed not on Si(111)-(7×7) but on a simplified Si(111)-(2×2) reconstruction.

Brommer *et al.*[20] have used DFT and the concept of local softness to study the interaction of foreign adatoms with the different dangling bonds of Si(111)-(7×7). For Pb adatoms, a preferential adsorption on faulted center adatoms and corner unfaulted adatoms was predicted. Finally, Staufer *et al.*[21] have performed extended Hückel calculations on the initial adsorption stages of Pb on Si(111)-(7×7) finding a preferential adsorption on the dangling bonds of the corner adatoms.

To clarify these issues, we have performed DFT calculations using both the local density approximation (LDA) (Ref. 22) and the generalized gradient approximation (GGA).[23] We used the SIESTA method,[24] with fully nonlocal[25] norm conserving pseudopotentials[26] and a basis set of numerical atomic orbitals[27] with double-ζ Si-s, Si-p, Pb-s, Pb-p valence orbitals and single-ζ Si-d and Pb-d polarization orbitals. Nonlinear partial-core exchange-correlation corrections were included in Pb's pseudopotential, which were thoroughly tested elsewhere.[28] A real-space integration grid with a plane wave cutoff of 100 Ry and a reciprocal k mesh[29]
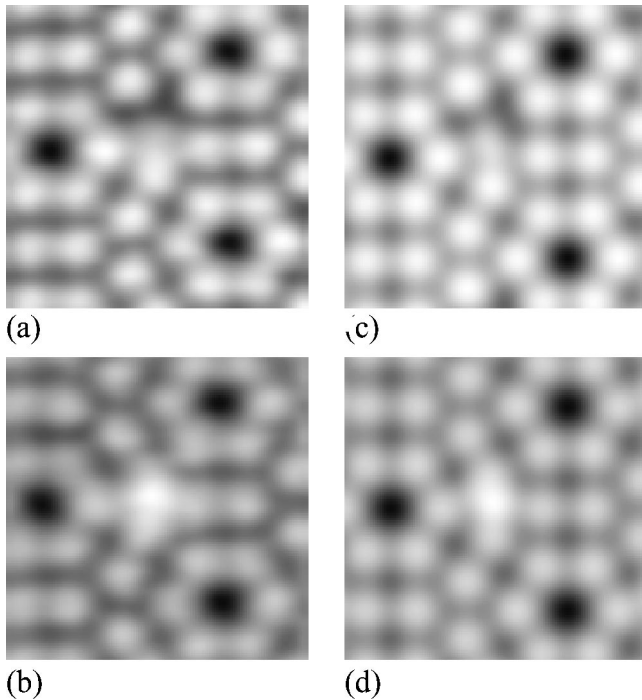
FIG. 4. Experimental [(a) and (b)] and theoretical [(c) and (d)] STM images for low bias [(a) and (c)] and high bias [(b) and (d)] conditions. Images (a) and (b) were measured at 93 K and at +0.5 V and +0.8 V sample bias. (c) and (d) are heights of an isosurface of the local density of states integrated between the Fermi level and +0.3 eV (c) and +0.8 eV (d).

FIG. 5. Arrhenius plots for jumps across basins of single Pb atoms adsorbed on faulted and unfaulted half cells.

with a cutoff[30] of 22 Å were used. All the geometries were relaxed, with a force tolerance of 0.04 eV/Å, in a slab geometry of four Si layers in addition to the Si adatoms, with the bottom layer fixed at crystalline positions and saturated by H atoms.

After placing a single Pb atom on different surface sites, the whole geometry was fully relaxed. First, we performed calculations on Si(111)-(2×2) reconstructions which mimic the unfaulted or faulted terraces [using a (4×4) supercell to separate the Pb adatoms]. The minimum energy was found for Pb adsorbed on one of the six B_2 sites located around a restatom [T_1 position, Fig. 3(b)]. These were the high-coordination sites also obtained for Si and Ge adsorption on Si(111)-(2×2).[18,19] The six sites would form a basin for adatom diffusion, with frequent jumps among them and much slower jumps between different basins. However, while in the (2×2) reconstruction all the B_2 sites are equivalent, their symmetry is broken in the (7×7) reconstruction, and this difference is essential to understand the experiments.

In Figs. 1 and 2, the Pb protrusions are not centered on T_1 positions, but they appear closer to center than to corner adatoms. This is perfectly accounted for by our calculations on the complete Si(111)-(7×7) dimer-adatom-stacking-fault reconstruction, in which there are three inequivalent B_2 sites [Fig. 3(b)]. The calculated absolute energy minimum is obtained for the $B_2(3)$ sites, which are closest to the center adatoms. The energy of the $B_2(1)$ and $B_2(2)$ sites is 0.09 eV
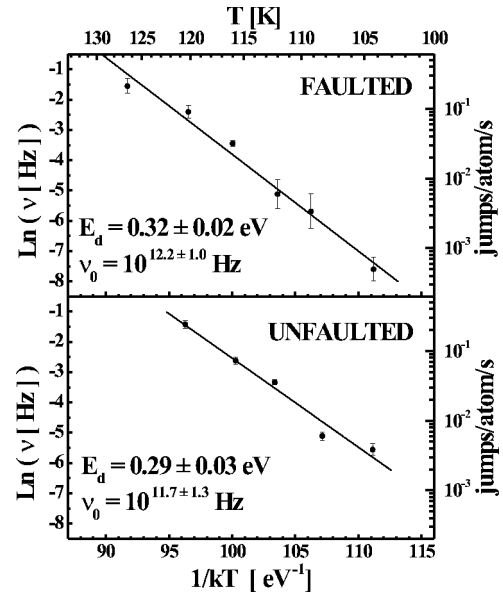
higher in both cases within the GGA (0.08 eV and 0.07 eV, respectively, within LDA). The T_1 site is much higher in energy (1.76 eV in LDA) so it can be completely discarded.

To increase our confidence for the identification of the Pb adsorption sites, we have simulated STM images with the Tersoff and Hammann approach[31] for Pb adsorbed on $B_2(3)$ sites. They are compared in Fig. 4 to the experimental images. The extremely good agreement at both low and high bias demonstrates that Pb adatoms are indeed adsorbed on $B_2(3)$ sites. Figures 2(b)–2(d) can also be completely understood under this light: they show single jumps between the two $B_2(3)$ sites inside a basin (b) to (c) and between different basins (c) to (d).

The energy barriers for intrabasin and interbasin jumps have also been calculated. Within the GGA they are 0.23 and 0.44 eV, respectively.[32] We have also measured these barriers with the STM, taking a great care to avoid tip-induced artifacts. It has been observed that a high bias can induce nonthermal Pb jumps both inside a basin and across basins of the same half cell.[33] At low bias (≤0.5 V) the situation is different for intrabasin and interbasin migration. While intrabasin jumps are still affected by the scanning process, interbasin jump rates can be measured safely at +0.5 V and 0.2 nA. Thus, by varying the temperature between 100 and 130 K, it was possible to measure the diffusion barrier across basins for both the faulted and the unfaulted half,[34] as shown in Fig. 5. The energy barriers were obtained from an Arrhenius fit of the form $\nu = \nu_0\, e^{-E_d/kT}$. The experimental interbasin barrier of 0.29±0.03 eV for the unfaulted half cells[35] compares reasonably well with the calculated one (0.44 eV).

In summary, we have performed a detailed analysis of single adatom adsorption and diffusion on Si(111)-(7×7) surfaces. The combination of first-principles calculations and variable temperature STM experiments have allowed us to unravel the complex dynamical behavior of a prototypical

*Email address: josem.gomez@uam.es

[1] L. Vitali, M. G. Ramsey, and F. P. Netzer, Phys. Rev. Lett. **83**, 316 (1999).

[2] M. Y. Lai and Y. L. Wang, Phys. Rev. B **64**, 241404(R) (2001).

[3] J.-L. Li, J.-F. Jia, X.-J. Liang, X. Liu, J.-Z. Wang, Q.-K. Xue, Z.-Q. Li, J. S. Tse, Z. Zhang, and S. B. Zhang, Phys. Rev. Lett. **88**, 066101 (2002).

[4] G. L. Kellog, Surf. Sci. Rep. **21**, 88 (1994).

[5] I. Štich, M. C. Payne, R. D. King-Smith, J.-S. Lin, and L. J. Clarke, Phys. Rev. Lett. **68**, 1351 (1992).

[6] K. D. Brommer, M. Needels, B. E. Larson, and J. D. Joannopoulos, Phys. Rev. Lett. **68**, 1355 (1992).

[7] F. Bechstedt, A. A. Stekolnikov, J. Furthmüller, and P. Käckell, Phys. Rev. Lett. **87**, 016103 (2001); A. A. Stekolnikov, J. Furthmüller, and F. Bechstedt, Phys. Rev. B **65**, 115318 (2002).

[8] C. M. Chang and C. M. Wei, Phys. Rev. B **67**, 033309 (2003).

[9] J. M. Gómez-Rodríguez, J. J. Sáenz, A. M. Baró, J.-Y. Veuillen, and R. C. Cinti, Phys. Rev. Lett. **76**, 799 (1996).

[10] J. M. Gómez-Rodríguez, J.-Y. Veuillen, and R. C. Cinti, J. Vac. Sci. Technol. B **14**, 1005 (1996).

[11] J. M. Gómez-Rodríguez, J.-Y. Veuillen, and R. C. Cinti, Surf. Rev. Lett. **4**, 335 (1997).

[12] T. Sato, S. Kitamura, and M. Iwatsuki, J. Vac. Sci. Technol. A **18**, 960 (2000).

[13] O. Custance, I. Brihuega, J. M. Gómez-Rodríguez, and A. M. Baró, Surf. Sci. **482-485**, 1406 (2001).

[14] J. Mysliveček, P. Sobotík, I. Ošt'ádal, T. Jarolímek, and P. Šmilauer, Phys. Rev. B **63**, 045403 (2001).

[15] C. Polop, E. Vasco, J. A. Martín-Gago, and J. L. Sacedón, Phys. Rev. B **66**, 085324 (2002).

[16] O. Custance, Ph.D. thesis, Universidad Autónoma de Madrid, 2002.

[17] R. Fernández, I. Horcas, P. Colilla, J.M. Gómez-Rodríguez, J. Colchero, J. Gómez-Herrero, and A.M. Baró (unpublished).

[18] K. Cho and E. Kaxiras, Europhys. Lett. **39**, 287 (1997).

[19] K. Cho and E. Kaxiras, Surf. Sci. **396**, L261 (1998).

[20] K. D. Brommer, M. Galván, A. Dal Pino, Jr., and J. D. Joannopoulos, Surf. Sci. **314**, 57 (1994).

[21] Ph. Sonnet, L. Stauffer, and C. Minot, Surf. Sci. **407**, 121 (1998).

[22] J. P. Perdew and A. Zunger, Phys. Rev. B **23**, 5048 (1981).

[23] J. P. Perdew, K. Burke, and M. Ernzerhof, Phys. Rev. Lett. **77**, 3865 (1996).

[24] P. Ordejón, E. Artacho, and J. M. Soler, Phys. Rev. B **53**, R10 441 (1996); J. M. Soler, E. Artacho, J. D. Gale, A. García, J. Junquera, P. Ordejón, and D. Sánchez-Portal, J. Phys.: Condens. Matter **14**, 2745 (2002).

[25] L. Kleinman and D. M. Bylander, Phys. Rev. Lett. **48**, 1425 (1982).

[26] N. Troullier and J. L. Martins, Phys. Rev. B **43**, 1993 (1991).

[27] J. Junquera, O. Paz, D. Sánchez-Portal, and E. Artacho, Phys. Rev. B **64**, 235111 (2001).

[28] S. Brochard, E. Artacho, O. Custance, I. Brihuega, A. M. Baró, J. M. Soler, and J. M. Gómez-Rodríguez, Phys. Rev. B **66**, 205403 (2002).

[29] H. J. Monkhorst and J. D. Pack, Phys. Rev. B **13**, 5188 (1976).

[30] J. Moreno and J. M. Soler, Phys. Rev. B **45**, 13 891 (1992).

[31] J. Tersoff and D. R. Hamann, Phys. Rev. Lett. **50**, 1998 (1983).

[32] According to LDA these barriers amount to 0.22 eV and 0.52 eV for intrabasin and interbasin jumps, respectively.

[33] O. Custance, I. Brihuega, A. M. Baró, and J. M. Gómez-Rodríguez (unpublished).

[34] The slight difference found between the barriers for faulted and unfaulted half cells is within the experimental error bars.

[35] All the calculations were performed for Pb adatoms adsorbed only on unfaulted half cells.